J. Fluid Mech. (1984), *vol.* 142, *pp.* 289–308
Printed in Great Britain

Shear dispersion and residence time for laminar flow in capillary tubes

By J. E. HOUSEWORTH

Environmental Engineering Science, California Institute of Technology, Pasadena, California 91125

(Received 30 June 1983 and in revised form 21 December 1983)

The behaviour of passive tracer particles in capillary Poiseuille flow is investigated with regard to the residence time in short axial sections of length z, in which $z/a < Va/D$, where a is the capillary radius, V is the mean velocity and D the coefficient of molecular diffusion. While methods exist for calculating moments of the cross-sectionally averaged axial concentration distribution as a function of time (e.g. Smith 1982*b*), much less is known about the distribution of residence time as a function of axial distance. An approximate theoretical solution for point sources in high-Péclet-number flows reveals that the mean residence time $\langle t(z)\rangle$, which is asymptotic to z/V_0 near the source, will then rise faster than z/V_0 before converging to z/V for large z, provided the source is not at the capillary wall. V_0 is the advective velocity at the point of release. The variance $\langle t^2(z)\rangle$ is found to increase initially in proportion to z^3 provided the source is not at the capillary wall or on the axis. A Monte Carlo method based on the solution to the diffusion equation in the capillary-tube cross-section is developed to compute particle trajectories which are used to analyse both axial and residence-time distributions. The residence-time distribution is found to display significant changes in character as a function of axial position, for both point sources and a uniform flux of particles along the tube.

1. Introduction

When passive tracer particles are introduced into Poiseuille flow, random lateral excursions caused by molecular diffusion coupled with the velocity profile cause an enhanced longitudinal dispersion. This phenomenon was first analysed by Taylor (1953), who provided a complete description of the asymptotic, cross-sectionally averaged axial concentration distribution. Since that time, Taylor's analysis has been applied to a wide variety of fluid-flow circumstances (Taylor 1954; Elder 1959; Saffman 1962; Fischer 1967). Taylor's (1953) analysis requires a certain initialization time $t > a^2/D$, where a is the tube radius and D the molecular diffusivity, before his results may be applied. In some cases, for example blood flow in arteries, there is interest in what happens for $t \ll a^2/D$ (Chatwin 1976). Most analytical and numerical work for the near-field problem has analysed the behaviour of the spatial concentration distribution as a function of time. In this paper, we will consider the variation in concentration over time as a function of axial position. We will limit our attention to small distances from the source, $z/a < Va/D$, where V is the mean velocity.

The results to be presented are principally devoted to cases where longitudinal molecular diffusion may be neglected. It is well known that, when the Péclet number $Pe = Va/D$ is large relative to 1, the longitudinal molecular diffusion is usually negligible. Chatwin (1976) shows for a source on the axis that if

$$Dt/a^2 \gg Pe^{-\frac{2}{3}} \tag{1.1}$$

then longitudinal molecular diffusion is negligible. This relationship is developed through scaling arguments which compare the amount of longitudinal spreading due to molecular diffusion versus differential advection. This reasoning may be extended for off-axis sources as follows. For a point source far from the axis and capillary wall, such that $(DT)^{\frac{1}{2}} \ll a - r_0$ and $(Dt)^{\frac{1}{2}} \ll r_0$, the velocity differential developed due to radial diffusion over distances of order $(Dt)^{\frac{1}{2}}$ is

$$\Delta V \sim \frac{V r_0}{a} \frac{(Dt)^{\frac{1}{2}}}{a}, \tag{1.2}$$

where r_0 is the radial location of the source. This leads to longitudinal spreading of order $t\Delta V$, while the longitudinal spreading due to molecular diffusion is of order $(Dt)^{\frac{1}{2}}$. For $t\Delta V \gg (Dt)^{\frac{1}{2}}$ we find

$$Dt/a^2 \gg (\eta_0 Pe)^{-1}, \tag{1.3}$$

where $\eta_0 = r_0/a$. Relation (1.3) also happens to be valid for a source at the wall, $r_0 = a$. For sources far from the capillary wall, $(Dt)^{\frac{1}{2}} \ll a - r_0$, we may scale t by z/V_0, where V_0 is the advective velocity at the source. For Poiseuille flow V_0 is of order $V(1-\eta_0^2)$. Substituting into (1.1) for t we find

$$z/a \gg Pe^{-\frac{1}{3}} \quad \text{if} \quad \eta_0 = 0. \tag{1.4}$$

For a source on the capillary wall, it is not possible to scale t by z/V_0 since $V_0 = 0$. For this case we scale t by $z/\Delta V$, where ΔV is given in (1.2) using $r_0 = a$. Using this in (1.3) we find

$$\frac{z}{a} \gg Pe^{-\frac{1}{2}} \quad \text{if} \quad \eta_0 = 1. \tag{1.5}$$

For intermediate values of η_0 the requirement on z may be constructed from (1.3), scaling t by z/V_0 to give

$$\frac{z}{a} \gg \frac{1-\eta_0^2}{\eta_0}, \tag{1.6}$$

which is valid if $(1-\eta_0)^2\eta_0^3 \gg Pe^{-1}$. Expressions (1.4)–(1.6) show when longitudinal molecular diffusion is negligible at a given distance z downstream of the source.

Consider a point source which instantaneously injects a small volume of tracer into high-Péclet-number flow in a capillary tube. At an observation point downstream of the source, we are able to detect the cross-sectionally averaged concentration of tracer $\bar{P}(z_{ob}, t)$, where z_{ob} is the axial distance of the observation station from the source and t is the time since source injection. Assume z_{ob}/a to be sufficiently large such that longitudinal molecular diffusion may be neglected. The concentration distribution $\bar{P}(z_{ob}, t)$ defines the probability density that a tracer particle will be at z_{ob} at time t. In addition, $\bar{P}(z_{ob}, t)$ is the probability density for a tracer particle to spend a time t in residence with $z \leqslant z_{ob}$. Suppose, for example, a radioactive substance is injected to irradiate a given length of the capillary tube. The residence-time distribution $\bar{P}(z_{ob}, t)$ would be needed to calculate the radiation dosage for a given distance downstream. Another example may be a chemical reaction which is desired to occur within a certain distance downstream of the source. In this case, a comparison of the residence time distribution with the reaction kinetics would be necessary.

A difficulty arises when longitudinal molecular diffusion is not negligible. Although $\bar{P}(z_{ob}, t)$ is still defined, it is not the residence time distribution. Through molecular diffusion, it is possible for a particle to move upstream. A particle that has passed the observation point z_{ob}, may diffuse upstream to $z < z_{ob}$ and again contribute to $\bar{P}(z_{ob}, t)$. The time t for this particle has not been spent entirely in the region $z \leqslant z_{ob}$, so $\bar{P}(z_{ob}, t)$ may not be considered a residence-time distribution in the sense given

above. The difference in interpretation of $\bar{P}(z_{ob}, t)$ takes on more significance when one considers a continuous or intermittent source rather than an instantaneous source. If $\bar{P}(z_{ob}, t)$ may be considered a residence-time distribution, it is the same regardless of whether the source is instantaneous, intermittent or continuous. This is not true when $\bar{P}(z_{ob}, t)$ is considered the tracer concentration.

Little work has been done to develop techniques for analysing $\bar{P}(z, t)$ as a residence-time distribution when $z/a \ll Pe$. Tsai & Holley (1978) derive temporal moment equations in a manner analogous to the moment method developed by Aris (1956). Through a numerical solution of the moment equations, they compare spatial and temporal moments for a tracer-concentration distribution in open-channel flow. In this paper we derive approximate analytical expressions for

$$\langle t(z)\rangle = \int_0^\infty t\bar{P}(z,t)\,\mathrm{d}t,$$

$$\langle t^2(z)\rangle = \int_0^\infty t^2\bar{P}(z,t)\,\mathrm{d}t - (\langle t(z)\rangle)^2,$$

which are derived under the condition that interaction between the tracer and the capillary wall are negligible. A Monte Carlo simulation of particle trajectories is developed to calculate moments of the residence time distribution and the full distribution $\bar{P}(z, t)$.

2. Governing equations

The governing equation for the probability density of a particle's position in Poiseuille flow is the advective diffusion equation, which in standard cylindrical coordinates is

$$\frac{\partial P}{\partial t} + u(r)\frac{\partial P}{\partial z} = D\left(\frac{\partial^2 P}{\partial z^2} + \frac{\partial^2 P}{\partial r^2} + \frac{1}{r}\frac{\partial P}{\partial r} + \frac{1}{r^2}\frac{\partial^2 P}{\partial \theta^2}\right). \tag{2.1}$$

The velocity profile is $u(r) = 2V(1-r^2/a^2)$, a is the tube radius, V is the mean velocity and D is the molecular diffusivity. Non-dimensionalizing (2.1), we find

$$\frac{\partial P}{\partial \hat{t}} + 2(1-\eta^2)\frac{\partial P}{\partial \hat{z}} = \frac{1}{(Pe)^2}\frac{\partial^2 P}{\partial \hat{z}^2} + \frac{\partial^2 P}{\partial \eta^2} + \frac{1}{\eta}\frac{\partial P}{\partial \eta} + \frac{1}{\eta^2}\frac{\partial^2 P}{\partial \theta^2}, \tag{2.2}$$

where

$$\hat{z} = \frac{Dz}{Va^2}, \quad \hat{t} = \frac{Dt}{a^2}, \quad \eta = \frac{r}{a}$$

and $Pe = Va/D$ is the Péclet number.

When concerned only with the axial distribution of the cross-sectionally averaged probability, (2.2) may be averaged over θ. In addition, we will limit the analysis to flows with high Péclet numbers, so longitudinal molecular diffusion may be ignored. Equation (2.2) becomes

$$\frac{\partial P^*}{\partial \hat{t}} + 2(1-\eta^2)\frac{\partial P^*}{\partial \hat{z}} = \frac{\partial^2 P^*}{\partial \eta^2} + \frac{1}{\eta}\frac{\partial P^*}{\partial \eta}, \tag{2.3}$$

where

$$P^* = \frac{1}{2\pi}\int_0^{2\pi} P\,\mathrm{d}\theta.$$

Equation (2.3) shows that the cross-sectionally averaged probability density is a function of $\hat{z}$ and $\hat{t}$ and the initial conditions.

When advection dominates longitudinal transport, the main effect of random molecular motion on the axial position of particles is through the coupling of lateral diffusion with the velocity profile. Taylor (1953) successfully investigated the asymptotic (far-field) behaviour of a passive tracer's cross-sectionally averaged axial concentration distribution by focusing on the interaction between lateral diffusion and the velocity profile. Transforming to a coordinate system moving with the mean flow, Taylor (1953) showed that the axial mass transport is proportional to the axial concentration gradient, which leads to an effective advective diffusion equation for the mean flow. No such simple transport equation exists for near-field advective diffusion, though attempts have been made to derive one (Smith 1982*a*). Numerical calculations for the near field (Gill & Ananthakrishnan 1967; Jayaraj & Subramanian 1978) have shown complex behaviour for the cross-sectionally averaged axial concentration distribution, which indicates that a numerical solution may be necessary to calculate the entire distribution. It is possible, though, to derive exact expressions for the mean and variance of the axial distribution which are valid for all distances from the source. These may be derived by taking moments of (2.2) (Aris 1956; Barton 1983), or by expanding the solution of (2.2) with orthogonal Hermite polynomials (Smith 1982*b*). Perhaps the most direct method is to use a technique due to Saffman (1960), which has been applied in the present context by Chatwin (1977), who derived approximate expressions for the axial mean and variance when $\hat{t} \ll 1$.

3. Analysis of averaged quantities

Let $\gamma(r, t; r_0)$ be the probability density for the radial position of a particle released at $r = r_0$, $t = 0$. Then the mean position may be calculated from (Saffman 1960; Chatwin 1977)

$$\langle V(\tau)\rangle = \int_0^a u(r)\,\gamma(r, \tau; r_0)\, r\, \mathrm{d}r, \tag{3.1}$$

$$\langle z(t)\rangle = \int_0^t \langle V(\tau)\rangle\, \mathrm{d}\tau \tag{3.2}$$

and the variance with respect to the mean (neglecting longitudinal molecular diffusion)

$$\langle V(\tau)\, V(\tau')\rangle = \int_0^a \int_0^a u(r)\, u(r')\, \gamma(r, \tau-\tau'; r')\, \gamma(r', \tau'; r_0)\, rr'\, \mathrm{d}r\, \mathrm{d}r', \tag{3.3}$$

$$\langle z^2(t)\rangle = 2\int_0^t \int_0^\tau \langle V(\tau)\, V(\tau')\rangle\, \mathrm{d}\tau'\, \mathrm{d}\tau - \langle z(t)\rangle^2. \tag{3.4}$$

Now $\gamma(r, t; r_0)$ is the solution of the diffusion equation in a circle with an initial 'ring' source, i.e.

$$\frac{\partial \gamma}{\partial t} = D\left(\frac{\partial^2 \gamma}{\partial r^2} + \frac{1}{r}\frac{\partial \gamma}{\partial r}\right), \tag{3.5}$$

with boundary and initial conditions

$$\frac{\partial \gamma}{\partial r} = 0 \quad \text{on} \quad r = a,$$

$$\gamma(r, 0; r_0) = \frac{1}{r_0}\delta(r - r_0),$$

where $\delta(r - r_0)$ is the Dirac delta function.

The solution for any initial axially symmetric distribution is well known (Crank 1956), and in this case gives

$$\gamma(r,t;r_0)=\frac{2}{a^2}\left\{1+\sum_{N=1}^{\infty}\exp(-\alpha_N^2 Dt)\frac{J_0(r\alpha_N)J_0(r_0\alpha_N)}{J_0^2(a\alpha_N)}\right\}, \tag{3.6}$$

where α_N is defined by $J_1(a\alpha_N)=0$, and J_0 and J_1 are Bessel functions of order 0 and 1. Using (3.6) and performing the integrals in (3.1)–(3.4), the mean and variance may be found to be (in dimensionless form)

$$\langle\hat{z}(\hat{t})\rangle=\hat{t}-8\sum_{N=1}^{\infty}[1-\exp(-\beta_N^2\hat{t})]\frac{J_0(\eta_0\beta_N)}{\beta_N^4 J_0(\beta_N)}, \tag{3.7}$$

$$\begin{aligned}\langle\hat{z}^2(\hat{t})\rangle &= 128\sum_{N=1}^{\infty}\beta_N^{-8}\{\hat{t}\beta_N^2-1+\exp(-\beta_N^2\hat{t})\}\\ &\quad-\frac{16}{3}\sum_{N=1}^{\infty}\{1-(1+\beta_N^2\hat{t})\exp(-\beta_N^2\hat{t})\}\frac{J_0(\eta_0\beta_N)}{\beta_N^6 J_0(\beta_N)}\\ &\quad+128\sum_{N=1}^{\infty}\sum_{m\neq N}\frac{(\beta_m^2+\beta_N^2)J_0(\eta_0\beta_N)}{(\beta_m^2-\beta_N^2)\beta_N^2\beta_m^4 J_0(\beta_N)}\left[1-\frac{\beta_m^2\exp(-\beta_N^2\hat{t})-\beta_N^2\exp(-\beta_m^2\hat{t})}{\beta_m^2-\beta_N^2}\right]\\ &\quad-64\left\{\sum_{N=1}^{\infty}[1-\exp(-\beta_N^2\hat{t})]\frac{J_0(\eta_0\beta_N)}{\beta_N^4 J_0(\beta_N)}\right\}^2,\end{aligned} \tag{3.8}$$

where $\beta_N=a\alpha_N$. Both (3.7) and (3.8) are given in Smith (1982*b*).

At first thought, one may reason that the average residence time in a section of length z_s may be found by inverting expression (3.7) to solve for t, with $\langle z(t)\rangle=z_s$. However, this does not give the mean residence time, but the time for the mean position to move a distance z_s. The mean and variance of the residence time distribution are

$$\langle t(z)\rangle=\int_0^{\infty}t\bar{P}(z,t)\,\mathrm{d}t, \tag{3.9}$$

$$\langle t^2(z)\rangle=\int_0^{\infty}t^2\bar{P}(z,t)\,\mathrm{d}t-\langle t(z)\rangle^2, \tag{3.10}$$

where

$$\bar{P}=\frac{2}{a^2}\int_0^a P^*(z,r,t)r\,\mathrm{d}r.$$

$\bar{P}$ is the cross-sectionally averaged probability density function for an instantaneous point source. $\bar{P}$ is normalized such that

$$\int_0^{\infty}\bar{P}(z,t)\,\mathrm{d}t=1. \tag{3.11}$$

For $\hat{t}>1$ we know Taylor's (1953) solution for $\bar{P}(\hat{z},\hat{t})$ applies (Chatwin 1970). Scaling t by z/V we see that $\hat{z}>1$ is needed for the asymptotic solution to be valid. Taylor's solution is

$$\bar{P}(\hat{z},\hat{t})=\frac{1}{(\frac{1}{12}\pi\hat{t})^{\frac{1}{2}}}\exp\left[\frac{-(\hat{z}-\hat{t})^2}{\frac{1}{12}\hat{t}}\right]. \tag{3.12}$$

Substituting (3.12) into (3.9) and (3.10) gives for the mean and variance

$$\langle\hat{t}(\hat{z})\rangle=\hat{z}+\tfrac{1}{24}, \tag{3.13}$$

$$\langle\hat{t}^2(\hat{z})\rangle=\tfrac{1}{24}\hat{z}+\tfrac{1}{288}. \tag{3.14}$$

As previously stated, an exact solution for $\bar{P}(\hat{z}, \hat{t})$ is not available when $\hat{z} \ll 1$, but an approximate solution for small times due to Chatwin (1976) may be used to investigate the initial behaviour of the residence time distribution. Chatwin's solution for a point source located at $r = r_0$ does not taken into account interaction between the tracer and the capillary wall, and is limited to $\hat{t} \ll (1-\eta_0)^2$. For $Pe \gg 1$ and $\hat{t} \ll (1-\eta_0)^2$, we scale t by z/V_0, which is of order $(z/V)(1-\eta_0^2)^{-1}$. Substituting, we find the restriction on $\hat{z}$ for Chatwin's solution to be

$$\hat{z} \ll (1-\eta_0^2)(1-\eta_0)^2. \tag{3.15}$$

Chatwin's (1976) approximate solution is

$$\bar{P}(z,t) = \frac{A}{\pi a^2} \frac{\exp[-(z-V_0 t)^2/4Dt]}{2(\pi Dt)^{\frac{1}{2}}} \times \left[1 - \frac{4Va}{D}\left(\frac{Dt}{a^2}\right)^{\frac{3}{2}} \frac{(z-V_0 t)}{2(Dt)^{\frac{1}{2}}} + \frac{8}{3}\left(\frac{V}{D}\right)^2 r_0^2 \left(\frac{Dt}{a^2}\right)^2 \left\{\frac{(z-V_0 t)^2}{2Dt} - 1\right\}\right]. \tag{3.16}$$

A is determined through normalization ((3.11)). Performing the integral in (3.9), and non-dimensionalizing the solution in terms of $\hat{z}$, η_0, V/V_0 and Pe, we find

$$\langle \hat{t}(\hat{z}) \rangle = \frac{V}{V_0}\hat{z}\left[1 + 12\left(\frac{V}{V_0}\right)^2 \hat{z} + 64\eta_0^2\left(\frac{V}{V_0}\right)^3 \hat{z} + 96\left(\frac{V}{V_0}\right)^3 \frac{1}{Pe^2} + 640\eta_0^2\left(\frac{V}{V_0}\right)^4 \frac{1}{Pe^2} + 2\frac{V}{V_0}\frac{1}{\hat{z}}\frac{1}{Pe^2} + 240\left(\frac{V}{V_0}\right)^4 \frac{1}{\hat{z}}\frac{1}{Pe^4} + 1920\eta_0^2\left(\frac{V}{V_0}\right)^5 \frac{1}{\hat{z}}\frac{1}{Pe^4}\right] \times \left[1 + 8\left(\frac{V}{V_0}\right)^2 \hat{z} + 32\eta_0^2\left(\frac{V}{V_0}\right)^3 \hat{z} + 24\left(\frac{V}{V_0}\right)^3 \frac{1}{Pe^2} + 128\eta_0^2\left(\frac{V}{V_0}\right)^4 \frac{1}{Pe^2}\right]^{-1}.$$

Now, considering the case where $Pe \to \infty$, we find

$$\langle \hat{t}(\hat{z}) \rangle = \frac{V}{V_0}\hat{z}\left\{\frac{1 + \left[12\left(\frac{V}{V_0}\right)^2 + 64\eta_0^2\left(\frac{V}{V_0}\right)^3\right]\hat{z}}{1 + \left[8\left(\frac{V}{V_0}\right)^2 + 32\eta_0^2\left(\frac{V}{V_0}\right)^3\right]\hat{z}}\right\}. \tag{3.17}$$

To neglect longitudinal diffusion for large but finite Péclet number, we have an additional restriction on $\hat{z}$ which is derived from (1.4) or (1.6), depending on the source position. These give restrictions on the downstream distance required such that longitudinal molecular diffusion is negligible. The complete set of restrictions on $\hat{z}$ for use of (3.17) are

$$\left.\begin{aligned} &\hat{z} \ll (1-\eta_0^2)(1-\eta_0)^2, \\ &\hat{z} \gg Pe^{-\frac{2}{3}} \quad \text{if} \quad \eta_0 = 0, \\ &\hat{z} \gg \frac{1-\eta_0^2}{\eta_0 Pe} \quad \text{if} \quad (1-\eta_0)^2 \eta_0^3 \gg Pe^{-1}. \end{aligned}\right\} \tag{3.18}$$

A more convenient non-dimensional representation of the mean residence time is $\langle \hat{t}(\hat{z}) \rangle = \langle Vt(z)/z \rangle = \langle \hat{t}(\hat{z}) \rangle / \hat{z}$, since this removes the bias that a longer section will have a larger residence time. A particle that moves with the mean velocity V will have a mean residence time $\langle \hat{t}(\hat{z}) \rangle = 1$ for any distance downstream. Using this scaling, we have

$$\langle \hat{t}(\hat{z}) \rangle = \frac{V}{V_0}\left\{\frac{1 + \left[12\left(\frac{V}{V_0}\right)^2 + 64\eta_0^2\left(\frac{V}{V_0}\right)^3\right]\hat{z}}{1 + \left[8\left(\frac{V}{V_0}\right)^2 + 32\eta_0^2\left(\frac{V}{V_0}\right)^3\right]\hat{z}}\right\}. \tag{3.19}$$

when $\hat{z} \ll (1-\eta_0^2)(1-\eta_0)^2$ and $Pe \to \infty$.

Through a comparison with numerical results (§6), we find for roughly 10% accuracy in $\langle \hat{t}(\hat{z}) \rangle$

$$\hat{z} \leqslant 0.1(1-\eta_0^2)(1-\eta_0)^2.$$

Plots of $\langle \hat{t}(\hat{z}) \rangle$ versus $\hat{z}$ are shown in figure 8. The initial behaviour of $\langle \hat{t}(\hat{z}) \rangle$ is to increase with increasing $\hat{z}$, regardless of the position of the source (provided the source is not at the wall). As an example, consider a source located at $\eta_0 = 0.8$ so that $V/V_0 = 1.39$. As $\hat{z} \to 0$ we see that $\langle \hat{t}(\hat{z}) \rangle \to V/V_0 = 1.39$. For $\hat{z} \to \infty$ we know $\langle \hat{t}(\hat{z}) \rangle \to 1$. Equation (3.19) predicts that $\langle \hat{t}(\hat{z}) \rangle$ will initially increase beyond 1.39 as $\hat{z}$ increases, before eventually decreasing to 1 as $\hat{z} \to \infty$. Further comments on the behaviour of the mean residence time will be given in §6, when Monte Carlo simulation results are compared with (3.19).

Integrating (3.16) for the variance and non-dimensionalizing as before gives

$$\begin{aligned}\langle \hat{t}(\hat{z}) \rangle = \left(\frac{V}{V_0}\right)^2 \hat{z}^2 \Bigg[& 1 + 16\left(\frac{V}{V_0}\right)^2 \hat{z} + \tfrac{320}{3}\eta_0^2 \left(\frac{V}{V_0}\right)^3 \hat{z} \\ & + 240\left(\frac{V}{V_0}\right)^3 \frac{1}{(Pe)^2} + 1920\eta_0^2 \left(\frac{V}{V_0}\right)^4 \frac{1}{(Pe)^2} + 6\left(\frac{V}{V_0}\right) \frac{1}{\hat{z}} \frac{1}{(Pe)^2} \\ & + 1440\left(\frac{V}{V_0}\right)^4 \frac{1}{\hat{z}} \frac{1}{(Pe)^4} + 13440\eta_0^2 \left(\frac{V}{V_0}\right)^5 \frac{1}{\hat{z}} \frac{1}{(Pe)^4} + 12\left(\frac{V}{V_0}\right)^2 \frac{1}{\hat{z}^2} \frac{1}{(Pe)^4} \\ & + 3360\left(\frac{V}{V_0}\right)^5 \frac{1}{\hat{z}^2} \frac{1}{(Pe)^6} + 35840\left(\frac{V}{V_0}\right)^6 \frac{1}{\hat{z}^2} \frac{1}{(Pe)^6} \Bigg] \\ & \times \left[1 + 8\left(\frac{V}{V_0}\right)^2 \hat{z} + 32\eta_0^2 \left(\frac{V}{V_0}\right)^3 \hat{z} + 24\left(\frac{V}{V_0}\right)^3 \frac{1}{(Pe)^2} + 128\eta_0^2 \left(\frac{V}{V_0}\right)^4 \frac{1}{(Pe)^2} \right]^{-1} - \langle \hat{t}(\hat{z}) \rangle^2.\end{aligned}$$

Taking the limit $Pe \to \infty$, we find

$$\langle \hat{t}^2(\hat{z}) \rangle = \tfrac{32}{3}\eta_0^2 \left(\frac{V}{V_0}\right)^5 \hat{z}^3 \Big/ \left\{ 1 + \left[16\left(\frac{V}{V_0}\right)^2 + 64\eta_0^2 \left(\frac{V}{V_0}\right)^3 \right] \hat{z} \right\}. \tag{3.20}$$

Note that at this level of approximation the first-order correction to the variance for a source on the axis ($\eta_0 = 0$) does not appear. Equation (3.20) is restricted to the range of $\hat{z}$ given in (3.18). In the following sections a Monte Carlo method is derived which solves (2.3) numerically. The method is used to calculate both axial distributions and residence-time distributions.

4. A Monte Carlo method for axial dispersion in Poiseuille flow

An approximate method for modelling the longitudinal motion of a particle in Poiseuille flow is to allow the particle to make a series of longitudinal steps for a fixed time step Δt. Neglecting axial molecular diffusion, the length of the ith longitudinal step is

$$\Delta z_i = u(r_i)\, \Delta t. \tag{4.1}$$

The key is to select r_i from the appropriate distribution for a given time step Δt, and previous radial coordinate r_{i-1}. This selection is governed by (3.6), which in this case is (in dimensionless form)

$$\gamma(\eta_i, \Delta\hat{t}; \eta_{i-1}) = \frac{2}{a^2} \left\{ 1 + \sum_{N=1}^{\infty} \exp(-\beta_N^2 \Delta\hat{t}) \frac{J_0(\eta_i \beta_N) J_0(\eta_{i-1} \beta_N)}{J_0^2(\beta_N)} \right\}. \tag{4.2}$$

Integrating equation (4.2) over the cross-section from 0 to η_i gives,

$$S(\eta_i, \Delta\hat{t}; \eta_{i-1}) = \eta_i^2 + 2\eta_i \sum_{N=1}^{\infty} \frac{\exp(-\beta_N^2 \Delta\hat{t})}{\beta_N} \frac{J_1(\eta_i \beta_N) J_0(\eta_{i-1} \beta_N)}{J_0^2(\beta_N)}, \tag{4.3}$$

where S is the cumulative probability distribution. For a fixed time step we invert (4.3) to give

$$\eta_i = g(S, \eta_{i-1}). \tag{4.4}$$

Since S is the cumulative probability distribution, it represents the probability that the new radial position of the particle will be less than or equal to η_i, given that the initial radial position is η_{i-1}. For a fixed η_{i-1}, S varies monotonically with η_i between $S(0) = 0$ and $S(1) = 1$. The probability that S will lie between any two values, say S_2 and S_1, is $|S_2 - S_1|$. Since the probability that S lies within any interval is equal to the size of the interval, S is uniformly distributed between 0 and 1.

The algorithm for each step is to generate a uniform random number for S and using η_{i-1} solve for η_i. Equation (4.1) may then be used to calculate the amount of axial motion for each time step. As to the selection of the time step, it is not possible to say *a priori* how large a step may be used, but the results can always be checked by the exact analytical results given by (3.7) and (3.8). Restrictions on the time step are based upon accuracy requirements since the solution is stable for any time step. We have found the time step $\Delta\hat{t} = 0.001$ to be sufficiently small for the calculations done here. Generating random values of η_i from (4.4) turns out to be too slow for practical calculations, so a large table of values has been computed, from which η_i could be accurately estimated by four-point interpolation. A grid of $g(201, 51)$ is used to approximate (4.4), the finer divisions in S being necessary since g changes rapidly near $S = 0$ and $S = 1$. Uniform random numbers are generated by combining two linear congruential random-number generators to produce a third 'ultra' random sequence. This technique, attributed to MacLaren and Marsaglia, is discussed in Knuth (1969). Axial and residence-time distributions are produced by computing simple histograms of the particle positions or times and filtering the resulting distribution with a numerical lopas filter, which removes high-frequency Monte Carlo 'noise' from the distribution.

The calculation procedure presented here may be extended to include longitudinal molecular diffusion. To do this, a stochastic longitudinal step Δz_{Di} is chosen from a Gaussian distribution with a mean of 0 and a variance $\sigma_z^2 = 2D\,\Delta t$. Equation (4.1) becomes

$$\Delta z_i = u(r_i)\,\Delta t + \Delta z_{Di}.$$

As stated in § 1, when longitudinal molecular diffusion is important at the observation point z_{ob}, $\bar{P}(z_{ob}, t)$ fails to qualify as a residence-time distribution. With the Monte Carlo technique, it is possible to calculate a residence-time distribution based on a definition suitable to the application. For example, if the distribution in time when particles first pass z_{ob} is desired, it is very easy to set up the Monte Carlo routine to do this.

In general, the Monte Carlo method described here is attractive when an analytical solution to the diffusion equation in the cross-section is available. Except for this restriction, the method is very flexible and can easily accommodate any velocity field or time-dependent phenomena. For example, it is possible to have an oscillating flow or flow through a converging–diverging tube, provided that the cross-section maintains a constant shape. The velocity field, which must be known for all positions and times, is always superimposed on the random motion. Turbulent flow may be modelled as well, if the assumption of a constant transverse turbulent diffusivity is used. Calculations for turbulent flow in tubes of circular cross-section may be done by changing from the laminar velocity profile to the mean turbulent velocity profile.

Source location	Dimensionless time $\hat{t}$	Monte Carlo average $\langle\hat{z}(\hat{t})\rangle$	Theoretical average $\langle\hat{z}(\hat{t})\rangle$	Monte Carlo variance $\langle\hat{z}^2(\hat{t})\rangle$	Theoretical variance $\langle z^2(\hat{t})\rangle$
0	0.01	0.01969	0.01960	0.9410 (−7)	0.1069 (−6)
0	0.05	0.09006	0.09031	0.6475 (−4)	0.6410 (−4)
0	0.10	0.1623	0.1622	0.7016 (−3)	0.7041 (−3)
0	0.20	0.2780	0.2784	0.003963	0.003949
0	0.30	0.3812	0.3822	0.008099	0.008079
0	0.50	0.5817	0.5833	0.01652	0.01648
0.67	0.01	0.01073	0.01072	0.4717 (−5)	0.4745 (−5)
0.67	0.05	0.05008	0.04997	0.3354 (−3)	0.3361 (−3)
0.67	0.10	0.09873	0.09849	0.001447	0.001443
0.67	0.20	0.1968	0.1973	0.004917	0.004845
0.67	0.30	0.2958	0.2970	0.008895	0.008816
0.67	0.50	0.4950	0.4969	0.01717	0.01709
1.0	0.01	0.002699	0.002714	0.2118 (−5)	0.2119 (−5)
1.0	0.05	0.02644	0.02643	0.1629 (−3)	0.1654 (−3)
1.0	0.10	0.06700	0.06691	0.8809 (−3)	0.8823 (−3)
1.0	0.20	0.1596	0.1603	0.003736	0.003711
1.0	0.30	0.2574	0.2588	0.007463	0.007458
1.0	0.50	0.4562	0.4584	0.01550	0.01564
AREA†	0.01	0.01005	0.01000	0.3108 (−4)	0.3177 (−4)
AREA	0.05	0.05023	0.05000	0.6146 (−3)	0.6295 (−3)
AREA	0.10	0.1003	0.1000	0.001975	0.002024
AREA	0.20	0.1994	0.2000	0.005627	0.005702
AREA	0.30	0.2986	0.3000	0.009614	0.009756
AREA	0.50	0.4979	0.5000	0.01779	0.01806

† Equivalent to an instantaneous source uniformly distributed over the cross-section

TABLE 1. Axial-distribution data

Everything else carries through as before, including the 'diffusion table' $g(S, \eta_{i-1})$. The calculations that produced $g(S, \eta_{i-1})$ are independent of the specific value of the diffusion coefficient (molecular or turbulent), owing to the dimensionless nature of (4.3).

The Monte Carlo method has been previously used in studies of turbulent diffusion (Kraichnan 1970), for longitudinal dispersion in turbulent open-channel flow (Sullivan 1971) and for longitudinal dispersion in laminar flows (Dewey & Sullivan 1982). The technique as presented here is somewhat different in that exact analytical results are used to model the random motions. It is essentially a numerical technique for solving (2.3). It is of some interest to see how well this technique can perform when no assumptions are involved and exact calculations are available for comparison. In addition, the Monte Carlo method has some advantages over standard numerical solution techniques. It contains no numerical dispersion, is absolutely stable, can exactly simulate delta-function sources in space and time, and is extremely simple to implement on a computer.

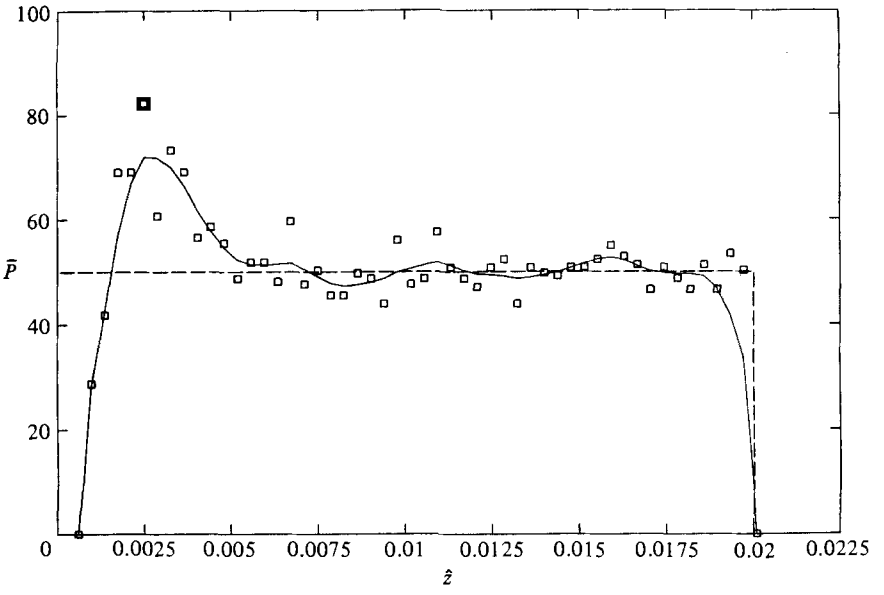

FIGURE 1. Axial distribution, area source: probability density $\bar{P}$ versus axial distance $\hat{z}$. □, Monte Carlo (unfiltered), 5000 particles; ——, Monte Carlo (filtered), – – – –, equation (5.2). $\hat{t} = 0.01$.

5. Results of calculations: axial profiles at a given time

Axial profiles provide an opportunity to check the calculations against the theoretical results given by (3.7) and (3.8) and with other numerical results. Table 1 summarizes the calculations for axial mean and variance, and is seen to be within 1 % for the mean and 2 % for the variance in most cases. Previous published works (Chatwin 1970; Gill & Ananthakrishnan 1967) have used an instantaneous spike source uniformly distributed over the cross-section as a characteristic example. To produce this type of initial distribution most easily, we would like to introduce particles uniformly over the cross-section in a random fashion (the AREA source in table 1). The probability for a particle to enter the tube at a given radius η within a differential range $\mathrm{d}\eta$ is in proportion to the differential area $\eta\,\mathrm{d}\eta$. Since the problem has axial symmetry, the initial angular position in the cross section is not important. The cumulative distribution is

$$S(\eta_0) = 2\int_0^{\eta_0} \eta\,\mathrm{d}\eta = \eta_0^2.$$

To select initial coordinates η_0 from the appropriate distribution, η_0 is chosen randomly as the square root of a uniformly distributed random number. Figure 1 shows the Monte Carlo calculations for a short time ($\hat{t} = 0.01$) after release of the tracer particles. Plotted along with this is the solution for pure advection, which in terms of the dimensionless variables $\hat{z}$ and $\hat{t}$ is (Chatwin 1970)

$$\bar{P}(\hat{z},\hat{t}) = \frac{1}{2\hat{t}} f((1-\hat{z}/2\hat{t})^{\frac{1}{2}}) \quad (0 \leqslant \hat{z} \leqslant 2\hat{t}),$$
$$\bar{P}(\hat{z},\hat{t}) = 0 \quad \text{otherwise}, \tag{5.1}$$

where $f(\eta)$ is the initial radial distribution of tracer at $\hat{t} = 0$ and $\hat{z} = 0$, subject to the condition

$$2\int_0^1 f(\eta)\,\eta\,\mathrm{d}\eta = 1.$$

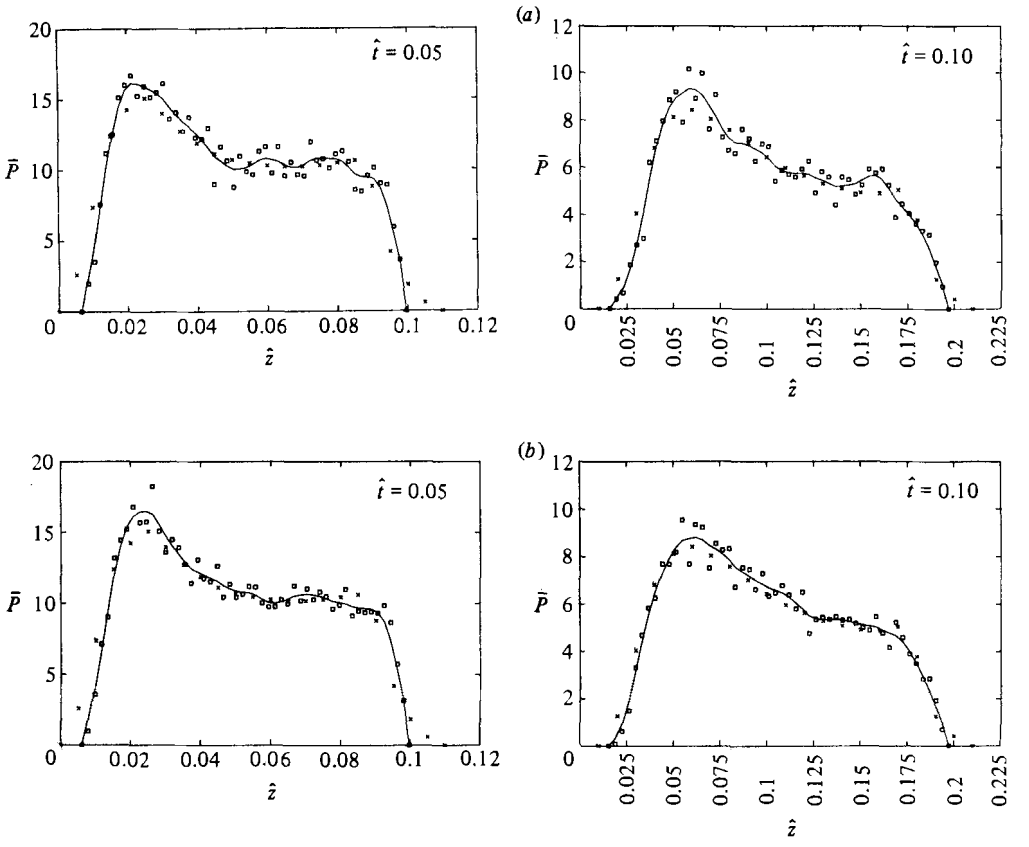

FIGURE 2. Axial distributions, area source: probability density $\bar{P}$ versus axial distance $\hat{z}$. □, Monte Carlo (unfiltered), (*a*) 5000 particles, (*b*) 10 000 particles; ——, Monte Carlo (filtered); ×, finite difference (Gill & Ananthakrishnan 1967).

For the present case $f(\eta) = 1$, and the pure-advection solution is

$$\left.\begin{aligned} \bar{P}(\hat{z},\hat{t}) &= \frac{1}{2\hat{t}} \quad (0 \leqslant \hat{z} \leqslant 2\hat{t}), \\ \bar{P}(\hat{z},\hat{t}) &= 0 \quad \text{otherwise.} \end{aligned}\right\} \tag{5.2}$$

The peak lagging the mean in figure 1 is in agreement with intuitive arguments put forward by Chatwin (1970) regarding the effects of preferential, radially inward, diffusion of particles initiated near the capillary wall. Figure 2(*a*) compares the finite-difference calculations of Gill & Ananthakrishnan (1967) with the current Monte Carlo calculations. The two calculations compare very closely, with the finite-difference solution showing slightly lower peak values with greater spreading at the tails of the distribution. These differences may be the result of inclusion of longitudinal molecular diffusion in the finite-difference calculations. As is evident from figures 1 and 2, the unfiltered Monte Carlo histogram contains a great deal of high-frequency noise which results from the estimation of a probability density function from a finite set of discrete samples. Figure 2(*b*) shows the effect of doubling the number of particles and indicates that the Monte Carlo solution is less reliable for high-frequency information. The various small 'bumps' in the filtered Monte Carlo solution should be considered residual noise which is passed through the lopas numerical filter. Figure 3 shows a

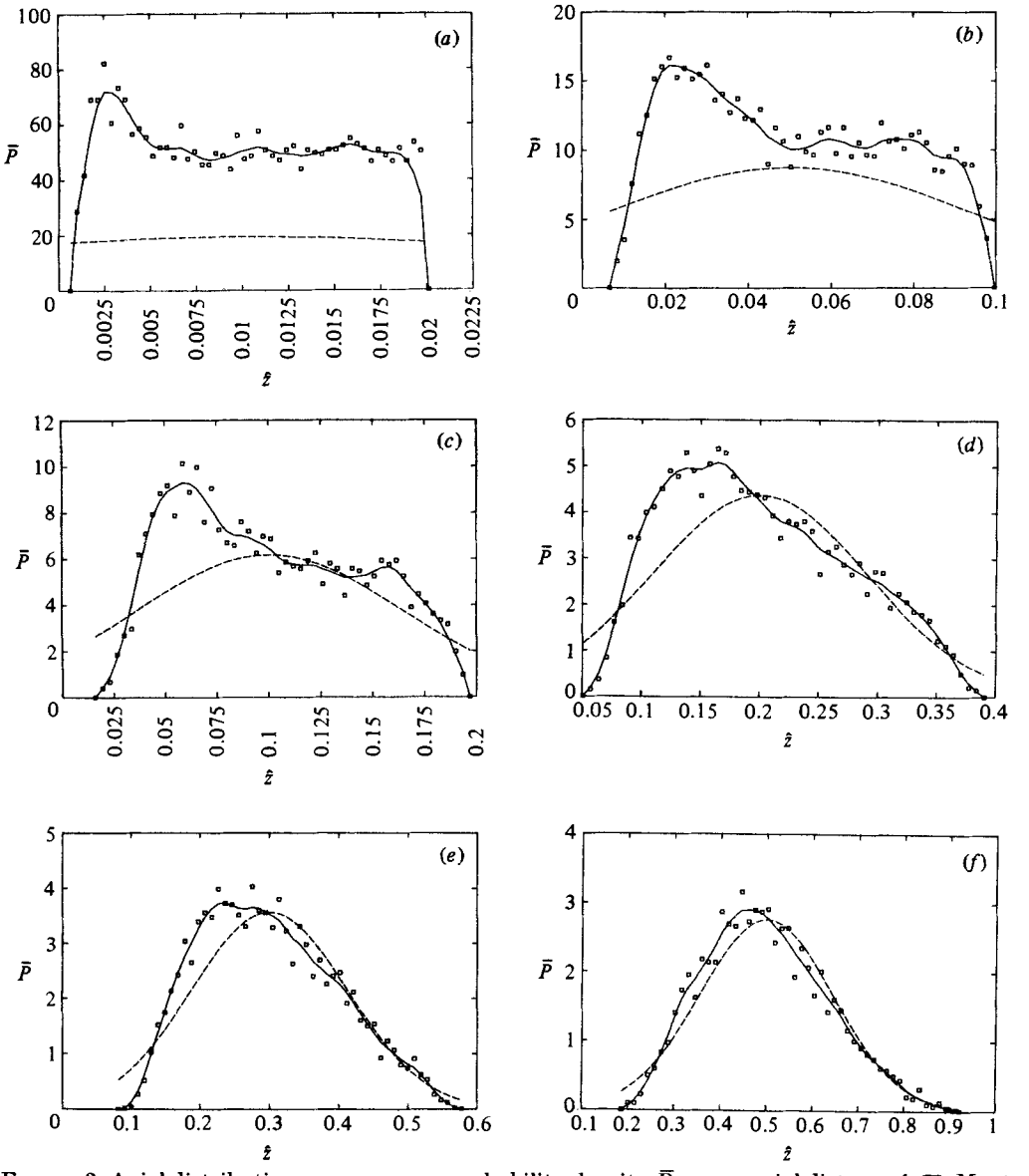

FIGURE 3. Axial distributions, area source: probability density $\bar{P}$ versus axial distance $\hat{z}$. □, Monte Carlo (unfiltered), 5000 particles; ——, Monte Carlo (filtered); – – – –, equation (3.12). Times: (*a*) $\hat{t} = 0.01$; (*b*) 0.05; (*c*) 0.10; (*d*) 0.20; (*e*) 0.30; (*f*) 0.50.

sequence of distributions from $\hat{t} = 0.01$ to $\hat{t} = 0.5$. Taylor's (1953) asymptotic Gaussian solution (3.12) is plotted along with the Monte Carlo solutions. The Monte Carlo distribution and the Gaussian solution are seen to match relatively well by the time $\hat{t} = 0.3$, which is in agreement with a prediction of Chatwin (1970) that the Gaussian limit is applicable beyond $\hat{t} = 0.25$.

The solution for the axial distribution from a point source at any initial radial position can also be calculated using the Monte Carlo technique. Figure 4 shows the progression of the axial distribution from an instantaneous point source with $\eta_0 = 0$. From table 1 it is seen that all the mean values have small error ($< 1\,\%$), while a

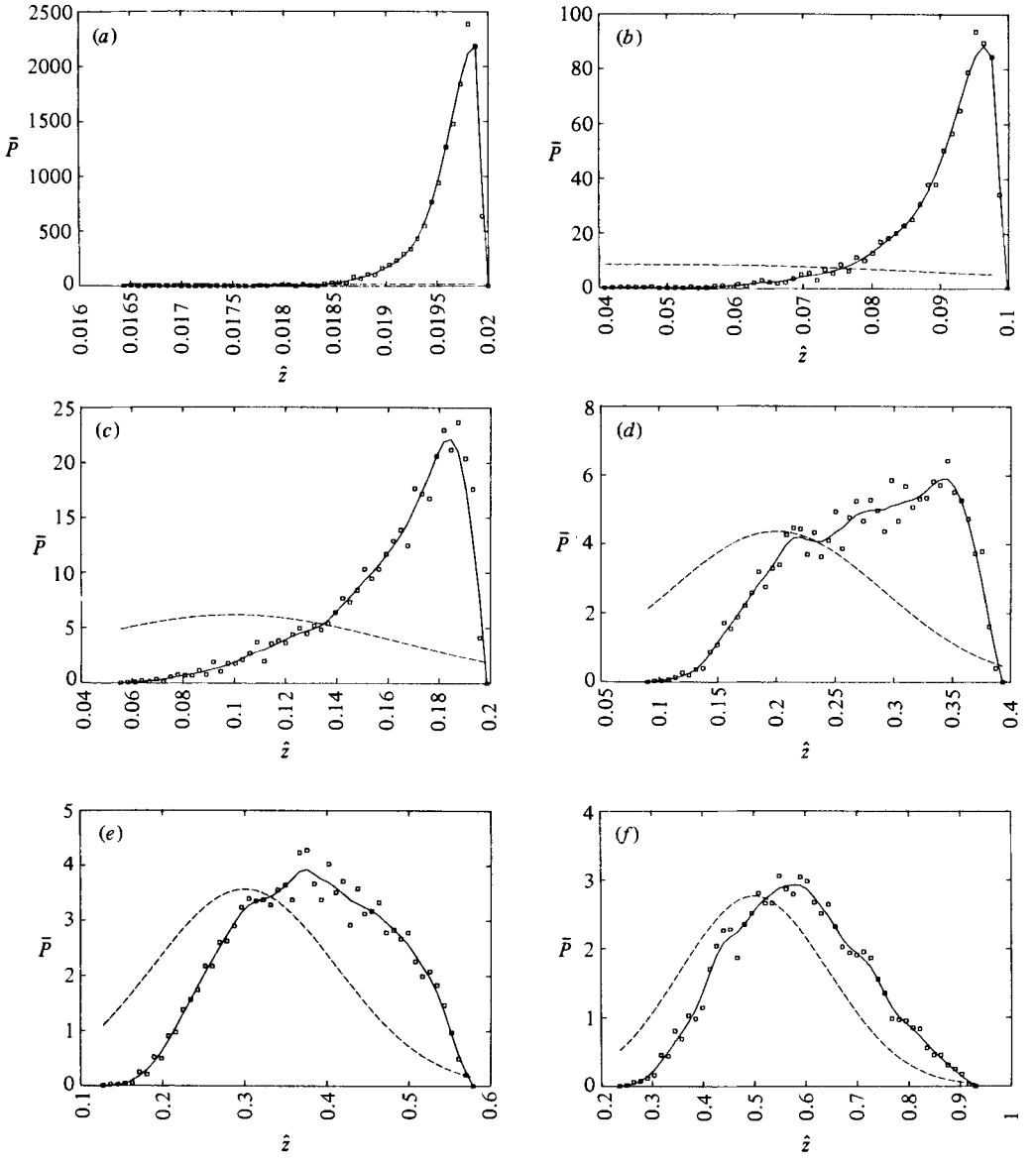

FIGURE 4. Axial distributions, point source, $\eta_0 = 0$: probability density $\bar{P}$ versus axial distance $\hat{z}$. □, Monte Carlo (unfiltered), 5000 particles; ——, Monte Carlo (filtered); – – – –, equation (3.12). Times: (*a*) $\hat{t} = 0.01$; (*b*) 0.05; (*c*) 0.10; (*d*) 0.20; (*e*) 0.30; (*f*) 0.50.

fairly large error occurs in the variance of the first distribution. This more substantial error is a result of the highly skewed shape of the distribution, for which a small error in representing its long tail results in a large error in the variance. As the distribution becomes more symmetric and approaches a Gaussian shape, errors in the variance are reduced. This is consistent with theoretical requirements that errors in the mean go to zero as $N^{-\frac{1}{2}}$ for any distribution, while errors in the variance are guaranteed to go to zero as $(\frac{1}{2}N)^{-\frac{1}{2}}$ only for a Gaussian distribution, N being the number of samples from the distribution (Hammersley & Handscomb 1964). The development of a 'knee' in the distribution at $\hat{t} = 0.2$ is a result of interaction between the capillary wall and

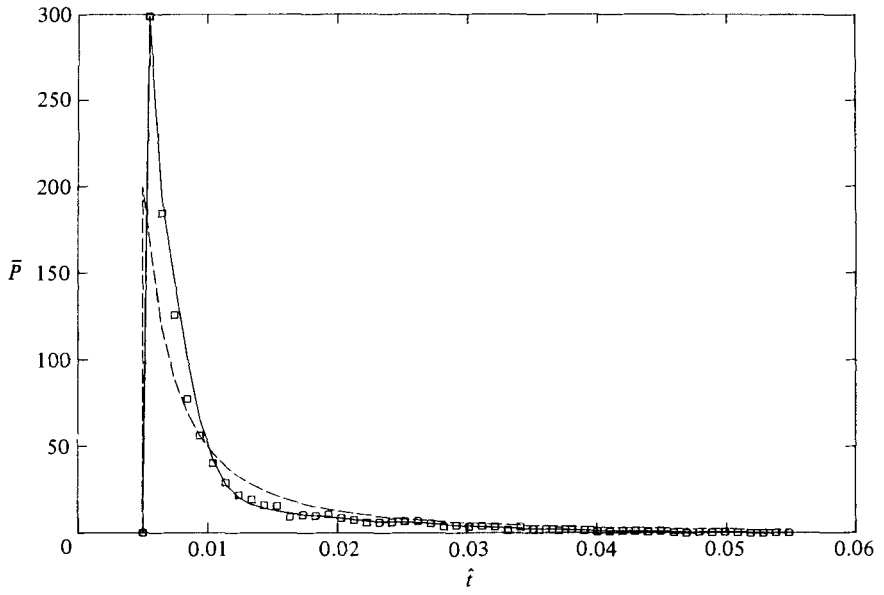

FIGURE 5. Residence-time distribution, flux source: probability density $\bar{P}$ versus residence time $\hat{t}$. □, Monte Carlo (unfiltered), 5000 particles; ——, Monte Carlo (filtered); – – – –, equation (6.2). $\hat{z} = 0.01$.

the radially diffusing tracer. At $\hat{t} = 0.1$ the capillary wall lies roughly 2.2 standard deviations from the source position, while at $\hat{t} = 0.2$ the wall is within 1.6 standard deviations. This means roughly 10 % of the particles have diffused to the wall when $\hat{t} = 0.2$, compared with about 2 % at $\hat{t} = 0.1$. Being unable to diffuse further out, the particles begin to migrate radially inward. The axial position of particles which have traversed the cross-section should be roughly equal to the cross-sectional mean velocity V times t, which in dimensionless terms means $\hat{z} = \hat{t}$. This closely corresponds to the location of the knee.

6. Results of calculations: residence-time distributions

Residence-time distributions provide the complement of axial distributions, being the distribution of the particle's probability density over time at a fixed location. This viewpoint is by far the most common in experimental work. Rather than introducing particles uniformly in the cross-section as we did for axial distributions, a more interesting problem is to allow particles to enter in proportion to the flux along a given streamline. This will model a uniform flux of tracer particles along the tube, where we are interested in the residence time for the particles in a particular axial section. For example, a well-mixed solution pumped through a short tube under steady-state conditions would be represented by this initial condition, neglecting end effects. The probability that a particle will enter the axial section at a given radius η within a differential range $\mathrm{d}\eta$ is $(1-\eta^2)\,\eta\,\mathrm{d}\eta$ (Saffman 1959). The cumulative distribution is

$$S(\eta_0) = 4\int_0^{\eta_0} (1-\eta^2)\,\eta\,\mathrm{d}\eta; \tag{6.1}$$

therefore

$$\eta_0^2 = 1-(1-S)^{\frac{1}{2}}.$$

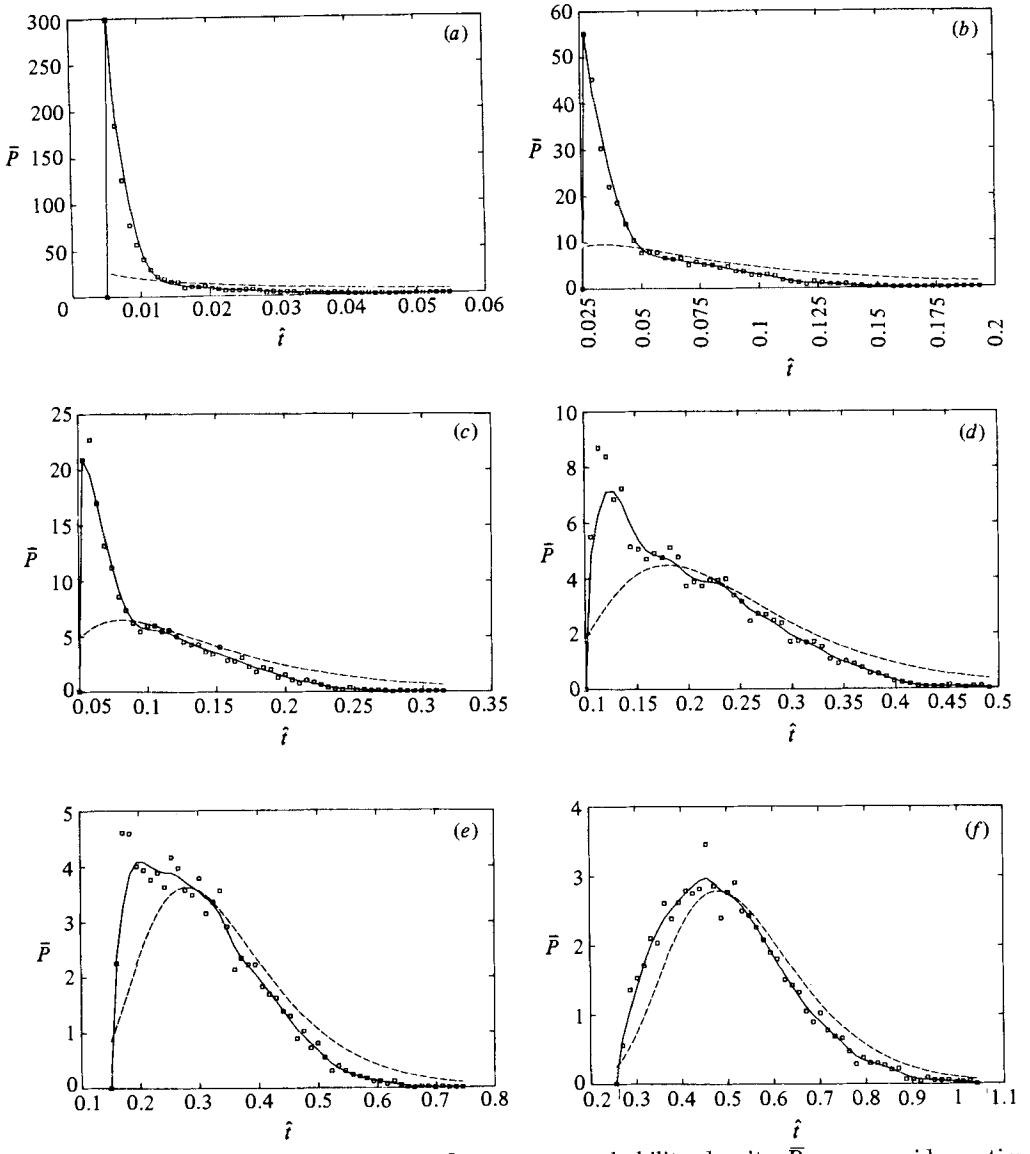

FIGURE 6. Residence-time distributions, flux source: probability density $\bar{P}$ versus residence time $\hat{t}$. □, Monte Carlo (unfiltered), 5000 particles; ——, Monte Carlo (filtered); – – – –, equation (3.12). Locations: (*a*) $\hat{z} = 0.01$; (*b*) 0.05; (*c*) 0.10; (*d*) 0.20; (*e*) 0.30; (*f*) 0.50.

Now if S is a uniform random number it has the same distribution as $1-S$ so

$$\eta_0 = (1-S^{\frac{1}{2}})^{\frac{1}{2}}.$$

Figure 5 shows the comparison of the pure-advection solution with Monte Carlo. From (6.1) it is seen that $f(\eta) = 2(1-\eta^2)$. Substituting into (5.1), we find for pure advection

$$\left.\begin{aligned} \bar{P}(\hat{z},\hat{t}) &= \frac{\hat{z}}{2\hat{t}^2} \quad (0 \leqslant \hat{z} \leqslant 2\hat{t}), \\ \bar{P}(\hat{z},\hat{t}) &= 0 \quad \text{otherwise.} \end{aligned}\right\} \tag{6.2}$$

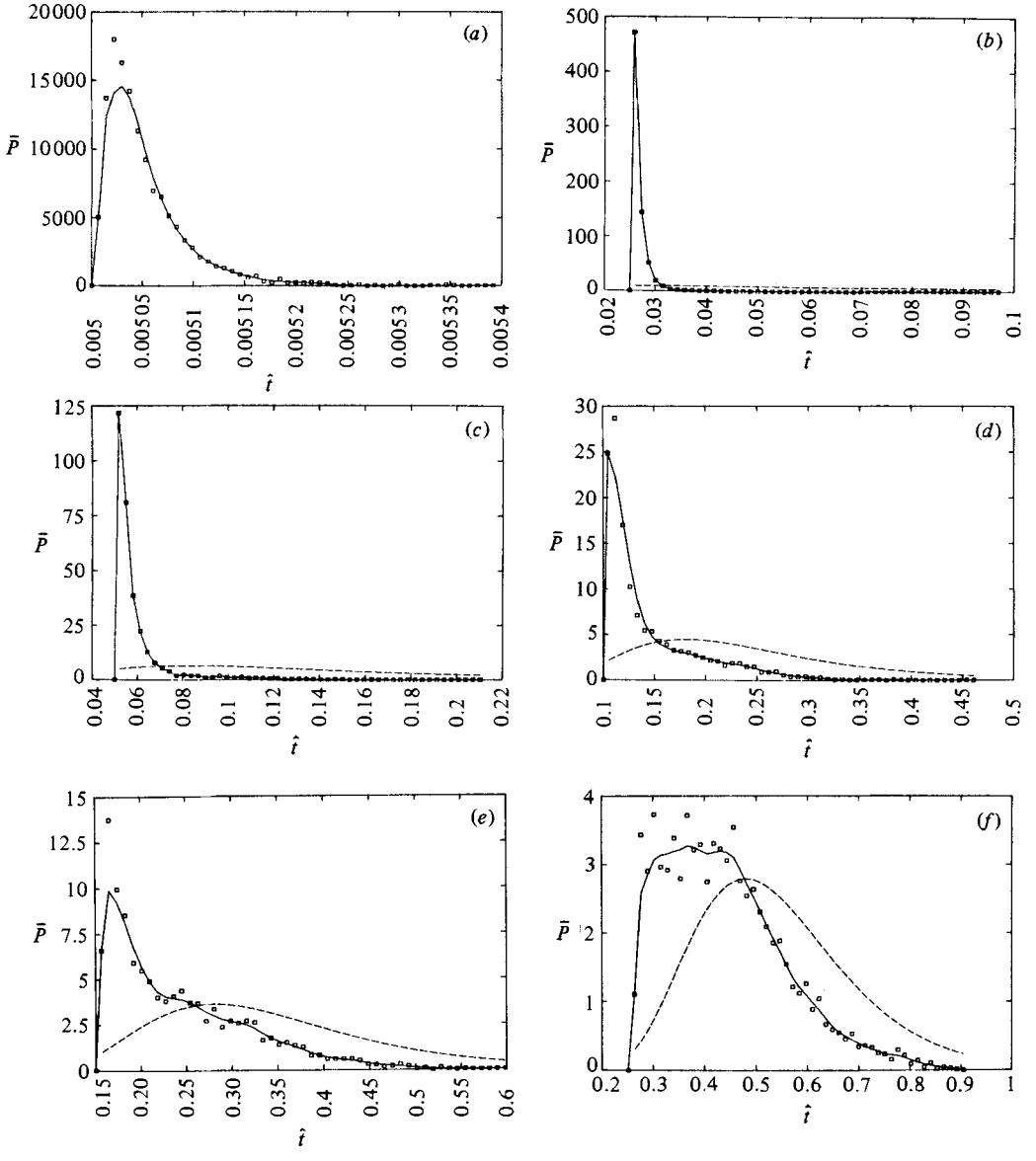

FIGURE 7. Residence-time distributions, points source, $\eta_0 = 0$: probability density, $\bar{P}$ versus residence time $\hat{t}$. □, Monte Carlo (unfiltered), 5000 particles; ——, Monte Carlo (filtered); – – – –, equation (3.12). Locations: (*a*) $\hat{z} = 0.01$; (*b*) 0.05; (*c*) 0.10; (*d*) 0.20; (*e*) 0.30; (*f*) 0.50.

Advection is seen to be the prime phenomenon that initially shapes the residence time distribution. Figure 6 shows the sequence of distributions starting at $\hat{z} = 0.01$ through $\hat{z} = 0.5$. Taylor's (1953) asymptotic solution (4.3) is again plotted along with the Monte Carlo solution. By $\hat{z} = 0.5$ the asymptotic solution is a reasonable approximation. Figure 7 shows the sequence of distributions from a point source at $\eta_0 = 0$ to successively more distant axial stations. Note the sharpening of the peak between $\hat{z} = 0.01$ and $\hat{z} = 0.05$. As in the case with a flux source, the residence-time distributions are skewed to the right, a feature found in all residence-time distributions investigated. Table 2 displays some statistical properties of the residence time

Source location	Dimensionless distance $\hat{z}$	Monte Carlo average $\langle \hat{t}(\hat{z}) \rangle$	Monte Carlo median $\hat{t}_{50}(\hat{z})$	Monte Carlo variance $\langle \hat{t}^2(\hat{z}) \rangle$
0	0.01	0.005052	0.005040	0.1700 (−8)
0	0.05	0.02661	0.02602	0.5200 (−5)
0	0.10	0.05919	0.05464	0.2061 (−3)
0	0.20	0.1437	0.1222	0.002274
0	0.30	0.2401	0.2180	0.005764
0	0.50	0.4375	0.4223	0.01401
0.67	0.01	0.01033	0.009178	0.1558 (−4)
0.67	0.05	0.05970	0.05021	0.7059 (−3)
0.67	0.10	0.1162	0.1071	0.002109
0.67	0.20	0.2215	0.2126	0.005130
0.67	0.30	0.3229	0.3123	0.009575
0.67	0.50	0.5245	0.5094	0.01829
1.0	0.01	0.02886	0.02737	0.1023 (−3)
1.0	0.05	0.09100	0.08736	0.8942 (−3)
1.0	0.10	0.1518	0.1477	0.002263
1.0	0.20	0.2598	0.2528	0.005764
1.0	0.30	0.3617	0.3546	0.009834
1.0	0.50	0.5641	0.5523	0.01850
FLUX†	0.01	0.009813	0.007144	0.4706 (−4)
FLUX	0.05	0.04920	0.03814	0.6995 (−3)
FLUX	0.10	0.09978	0.08323	0.002117
FLUX	0.20	0.1996	0.1846	0.005534
FLUX	0.30	0.2997	0.2850	0.009631
FLUX	0.50	0.5006	0.4833	0.01835

† Equivalent to a steady-state uniformly mixed source of particles entering the capillary tube

TABLE 2. Residence-time distribution data

distributions calculated with the Monte Carlo model. The median residence time, $\hat{t}_{50}(\hat{z})$ in table 2, is the time for 50% of the particles to pass the downstream position $\hat{z}$. For the uniform 'flux' case at the nearest station ($\hat{z} = 0.01$), the residence-time distribution is highly skewed, having 50% of the particles pass through the section in a time roughly 30% less than the mean residence time. As the distance to the downstream section increases, the median moves closer to the mean (in a relative sense) and the distribution becomes more symmetric.

The mean residence time as a function of axial distance for various source positions is shown in figure 8. The mean residence time here is non-dimensionalized as $\langle \dot{t}(\hat{z}) \rangle = \langle Vt(z)/z \rangle = \langle \hat{t}(\hat{z}) \rangle / \hat{z}$. The approximate theoretical solution (3.19) obtained earlier is shown with the Monte Carlo solution. The approximate solution is seen to maintain roughly 10% accuracy if $\hat{z} \leqslant 0.1(1-\eta_0^2)(1-\eta_0)^2$. Since the dimensionless mean residence time $\langle \dot{t}(\hat{z}) \rangle$ will always initially rise (except for a source at the wall), and since $\langle \dot{t}(\hat{z}) \rangle \to 1$ as $\hat{z} \to \infty$, particles starting out on streamlines slower than the mean velocity must necessarily display a maximum at some intermediate $\hat{z}$. As it turns out, particles started on streamlines somewhat faster than the mean also display this maximum behaviour since the initial rise in the mean residence time may exceed 1.

The initial rise in mean residence time is intuitively easy to understand. Consider a linear velocity profile with a continuous point source of tracer material being measured at a fixed downstream station. Particles diffusing into the lower velocity

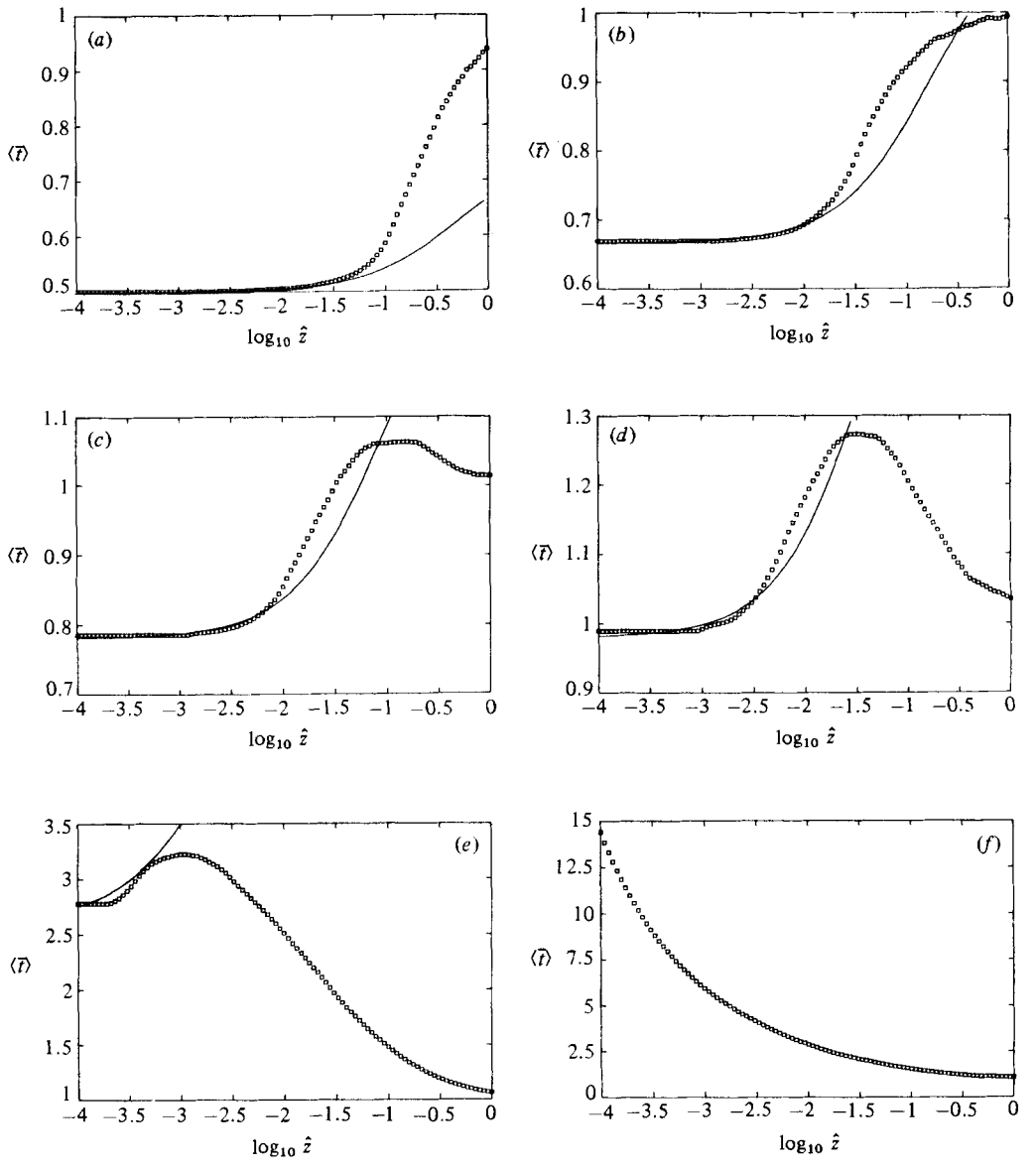

FIGURE 8. Mean residence time $\langle \bar{t}(\hat{z}) \rangle$ versus $\log_{10} \hat{z}$. □, Monte Carlo (unfiltered), 2000 particles; ——, equation (3.19). Locations: (*a*) $\eta_0 = 0$; (*b*) 0.5; (*c*) 0.6; (*d*) 0.7; (*e*) 0.9; (*f*) 1.0.

region will take longer to pass by the downstream station and hence will have more time to diffuse laterally, allowing some particles to sample even lower axial velocities. Particles diffusing into the higher-velocity zone are more rapidly swept by the downstream station and do not have as much time to diffuse laterally. This asymmetry causes the initial rise in mean residence time, with the boundary preventing further increase.

7. Conclusions

Theoretical studies of near-field advective diffusion have been successful in analysing some of the features of the cross-sectionally averaged axial distribution. A Monte Carlo method is used here to investigate some of the important features of the residence-time distribution for both point and uniform sources. The residence-time distribution is shown to change from a highly skewed character to a more symmetric form with increasing axial distance for both point sources and a uniform flux of particles along the tube. All residence-time distributions maintain the same sense to their skewness in that the median always lies at a smaller time than the mean, which in short sections can be quite pronounced. The dimensionless mean residence time $\langle \hat{t}(\hat{z}) \rangle$ displays a maximum as a function of downstream distance for point sources located approximately between $\eta_0 = 0.6$ and $\eta_0 < 1$. Through integration of an approximate theoretical solution due to Chatwin (1976), the mean and variance of the residence-time distribution are found for $\hat{z} \ll 1$. For a point source located at η_0, $0 < \eta_0 < 1$, the variance $\langle \hat{t}^2(\hat{z}) \rangle$ is found to increase initially in proportion to $\hat{z}^3$ before converging to an asymptotic growth rate proportional to $\hat{z}$. The dimensionless mean residence time $\langle \hat{t}(\hat{z}) \rangle$ is found to rise initially with increasing downstream distance for any point source in the cross-section, with the exception of a point source at the capillary wall. This phenomenon is in agreement with the Monte Carlo calculations and with intuitive reasoning.

The support and encouragement of Professor Norman Brooks is gratefully acknowledged. This research is funded by the Caltech Environmental Quality Laboratory through support from Andrew W. Mellon Foundation.

REFERENCES

ARIS, R. 1956 On the dispersion of a solute in a fluid flowing through a tube. *Proc. R. Soc. Lond.* A **235**, 67.

BARTON, N. G. 1983 On the method of moments for solute dispersion. *J. Fluid Mech.* **126**, 205.

CHATWIN, P. C. 1970 The approach to normality of the concentration distribution of a solute in a solvent flowing along a straight pipe. *J. Fluid Mech.* **43**, 321.

CHATWIN, P. C. 1976 The initial dispersion of contaminant in Poiseuille flow and the smoothing of the snout. *J. Fluid Mech.* **77**, 593.

CHATWIN, P. C. 1977 The initial development of longitudinal dispersion in straight tubes. *J. Fluid Mech.* **80**, 33.

CRANK, J. 1956 *The Mathematics of Diffusion.* Oxford University Press.

DEWEY, R. J. & SULLIVAN, P. J. 1982 Longitudinal-dispersion calculations in laminar flows by statistical analysis of molecular motions. *J. Fluid Mech.* **125**, 203.

ELDER, J. W. 1959 The dispersion of marked fluid in turbulent shear flow. *J. Fluid Mech.* **5**, 554.

FISCHER, H. B. 1967 The mechanics of dispersion in natural waters. *J. Hydraul. Div. ASCE* **93**, 187.

GILL, W. N. & ANANTHAKRISHNAN, V. 1967 Laminar dispersion in capillaries: part 4. The slug stimulus. *AIChE J.* **13**, 801.

HAMMERSLEY, J. M. & HANDSCOMB, D. C. 1979 *Monte Carlo Methods.* Chapman & Hall.

JAYARAJ, K. & SUBRAMANIAN, R. SHANKAR 1978 On relaxation phenomena in field-flow fractionation. *Sep. Sci. Tech.* **13**, 791.

KNUTH, D. E. 1969 *Seminumerical Algorithms – The Art of Computer Programming*, vol. 2. Addison-Wesley.

KRAICHNAN, R. H. 1970 Diffusion by a random velocity field. *Phys. Fluids* **13**, 22.

SAFFMAN, P. G. 1959 A theory of dispersion in a porous medium. *J. Fluid Mech.* **6**, 321.

SAFFMAN, P. G. 1960 On the effect of the molecular diffusivity in turbulent diffusion. *J. Fluid Mech.* **8**, 273.

SAFFMAN, P. G. 1962 The effect of wind shear on horizontal spread from an instantaneous ground source. *Q. J. R. Met. Soc.* **88**, 382.

SMITH, R. 1982*a* Non-uniform discharges of contaminants in shear flows. *J. Fluid Mech.* **120**, 71.

SMITH, R. 1982*b* Gaussian approximation for contaminant dispersion. *Q. J. Mech. Appl. Math.* **35**, 345.

SULLIVAN, P. J. 1971 Longitudinal dispersion within a two-dimensional turbulent shear flow. *J. Fluid Mech.* **49**, 551.

TAYLOR, G. I. 1953 Dispersion of soluble matter in solvent flowing slowly through a tube. *Proc. R. Soc. Lond.* A **219**, 186.

TAYLOR, G. I. 1954 The dispersion of matter in turbulent flow through a pipe. *Proc. R. Soc. Lond.* A **223**, 446.

TSAI, Y. H. & HOLLEY, E. R. 1978 Temporal moments for longitudinal dispersion. *J. Hydraul. Div. ASCE* **12**, 1617.